

AD-A253 701



OFFICE OF NAVAL RESEARCH

Grant N00014-90-J-1193

TECHNICAL REPORT No. 90

DTIC
ELECTE
AUG 4 1992
S C D

2

Internal Explosion in Laser Ablation of Superconducting Targets

by

D. L. Lin, X. Li, Z. D. Liu and Thomas F. George

Prepared for publication

in

Journal of Applied Physics

Departments of Chemistry and Physics
Washington State University
Pullman, WA 99164-1046

July 1992

Reproduction in whole or in part is permitted for any purpose of the United States Government.

This document has been approved for public release and sale; its distribution is unlimited.

92 7 31 126

92-20841



REPORT DOCUMENTATION PAGE

Form Approved
OMB No. 0704-0188

Please reporting burden for this collection of information is estimated to average 1 hour per response, including the time for reviewing instructions, searching existing data sources, gathering and maintaining the data needed, and completing and reviewing the collection of information. Send comments regarding this burden estimate or any other aspect of this collection of information, including suggestions for reducing this burden, to Washington Headquarters Services, Directorate for Information Operations and Reports, 1215 Jefferson Davis Highway, Suite 1204, Arlington, VA 22202-4302, and to the Office of Management and Budget, Paperwork Reduction Project (0704-0188), Washington, DC 20503.

1. AGENCY USE ONLY (Leave blank)		2. REPORT DATE July 1992		3. REPORT TYPE AND DATES COVERED Interim	
4. TITLE AND SUBTITLE Internal Explosion in Laser Ablation of Superconducting Targets				5. FUNDING NUMBERS Grant N00014-90-J-1193	
6. AUTHOR(S) D. L. Lin, X. Li, Z. D. Liu and <u>Thomas F. George</u>					
7. PERFORMING ORGANIZATION NAME(S) AND ADDRESS(ES) Departments of Chemistry and Physics Washington State University				8. PERFORMING ORGANIZATION REPORT NUMBER WSU/92/90	
9. SPONSORING/MONITORING AGENCY NAME(S) AND ADDRESS(ES) Office of Naval Research 800 N. Quincy Street Arlington, Virginia 22217				10. SPONSORING/MONITORING AGENCY REPORT NUMBER	
11. SUPPLEMENTARY NOTES Prepared for publication in <u>Journal of Applied Physics</u>					
12a. DISTRIBUTION/AVAILABILITY STATEMENT Approved for public release; distribution unlimited				12b. DISTRIBUTION CODE	
13. ABSTRACT (Maximum 200 words) The temperature profile inside a superconducting target in laser ablation is calculated for laser pulses of various shapes. The calculation is based on the equation of heat conduction. All parameters characterizing the target material are assumed to be temperature dependent and are determined empirically by extrapolating experimental data to the melting point. The receding velocity of the vapor-solid interface is determined by the dynamical balance of energy. Our calculation shows that, in general, there exist subsurface overheating spots at different instants as long as the laser pulse intensity is strong enough. The dependence of their occurrence on the pulse shape is analyzed, and conditions to avoid them without jeopardizing the deposition process are discussed.					
14. SUBJECT TERMS LASER ABLATION SUPERCONDUCTING TARGETS INTERNAL EXPLOSION VAPOR-SOLID INTERFACE TEMPERATURE PROFILE SUBSURFACE OVERHEATING				15. NUMBER OF PAGES 21 16. PRICE CODE NTIS	
17. SECURITY CLASSIFICATION OF REPORT Unclassified	18. SECURITY CLASSIFICATION OF THIS PAGE Unclassified	19. SECURITY CLASSIFICATION OF ABSTRACT Unclassified	20. LIMITATION OF ABSTRACT		

Internal explosion in laser ablation of superconducting targets

D. L. Lin, X. Li and Z. D. Liu

Department of Physics and Astronomy

State University of New York at Buffalo

Buffalo, New York 14260

Thomas F. George

Departments of Chemistry and Physics

Washington State University

Pullman, Washington 99164-1046

Abstract

The temperature profile inside a superconducting target in laser ablation is calculated for laser pulses of various shapes. The calculation is based on the equation of heat conduction. All parameters characterizing the target material are assumed to be temperature dependent and are determined empirically by extrapolating experimental data to the melting point. The receding velocity of the vapor-solid interface is determined by the dynamical balance of energy. Our calculation shows that, in general, there exist subsurface overheating spots at different instants as long as the laser pulse intensity is strong enough. The dependence of their occurrence on the pulse shape is analyzed, and conditions to avoid them without jeopardizing the deposition process are discussed.

PACS numbers: 74.75.+t, 66.70.+f, 81.60Dq, 81.90.+c

Accession For

DTIC SERIAL ☒

DTIC REF ☐

Unannounced ☐

Justification

By

Distribution/

Availability Codes

Avail and/or

Dist

Special

A-1

DTIC QUALITY INSPECTED S

I. Introduction

The discovery of high- T_c superconductivity has prompted numerous efforts in the preparation of high-quality superconducting thin films. Among many successful techniques to date, such as sputtering,¹ thermal and electron beam evaporation,² molecular deposition³ and sol-gel,⁴ the pulsed laser deposition (PLD)⁵ ^{has} its unique advantages. The PLD technique is relatively inexpensive, and provides high deposition rates and excellent control of ^{the} stoichiometry of the deposited film. It even eliminates the post-annealing procedure. Furthermore, the low chamber pressure during the deposition process reduces the undesirable impurities.

Much progress has been made recently. For example, Y-Ba-Cu-O/ Y_x -Pr_{1-x}-Ba-Cu-O superlattices have been successfully grown by the PLD technique.⁶ Techniques are also greatly advanced in the fabrication of controllable Josephson junctions⁷ and in the growth of thin films of YBaCuO (YBCO) onto the new magnetic substrate⁸ YbFeO₃. The chamber temperature during the PLD process, however, has to be greatly reduced if the technique is applied in the integration of superconductors and semiconductors for device purposes. This is because most semiconductors can not tolerate temperatures higher than 450°C. The introduction of an oxygen jet into the laser-ablated plasma has made it possible to process superconducting thin films at 650°C. Further reductions in temperature have been reported by the incorporation of an oxygen plasma.⁹ A new technique involving plasma-assisted laser deposition has been developed to fabricate superconducting YBCO films without post-annealing.¹⁰

The quality of superconducting films made in the PLD process depends on a number of factors such as the energy density, wavelength, duration and shape of the laser pulse, the incident angle, the optical and thermal properties of the pellet, and the distance between the pellet and the substrate. As a matter of fact, the PLD process consists of three stages: 1) laser evaporation (LE) of the superconducting target, 2) transport of the evaporated material from the target to the substrate and 3) deposition on the substrate. The evaporated material may be atoms, ions, molecules and clusters, and the presence of large molecules and clusters eventually influences the film quality. The transport process is most complicated to control experimentally and most difficult to treat theoretically. Particles of various sizes and charges move in an oxygen-filled chamber exposed to laser pulses, and hence collisions of all types are involved in this stage. The final stage involves the deposition of all particles including products of chemical reactions during the transport.

Attempts have been made to understand the nature of these processes. The angular distribution of the composition and thickness of the YBCO film has been measured.¹¹ It appears that there exist two distinct components in the deposited material. One is the nonstoichiometric $\cos\theta$ component, where θ is the angle with respect to the normal to the substrate surface, and the other is the stoichiometric forward-directed component. An anisotropic expansion of the high-pressure laser-evaporated plasma has been suggested to explain such spatial variations in the deposition.¹² During the LE process, a partially-ionized plasma has been observed above the target surface,¹³ and high-energy atomic beams¹⁴ and cluster emission¹⁵ have also been found in

experiments. Besides, it is known experimentally that the pulse duration plays an important role in the final film quality.¹⁶

On the other hand, much less theoretical research has been conducted to understand the complex mechanism governing the PLD. A model was developed with predictions in qualitative agreement with experiments.¹⁷ It assumes that a high-temperature plasma is created out of the evaporated material under the irradiation by the laser pulse. An adiabatic expansion of the plasma then results in the deposition. The treatment of the first stage of LE, however, is oversimplified in this model, so that it fails to provide the temperature profile of the target. The change of temperature with time and depth in the target is necessary to investigate the possibility of explosion,¹⁸ since liquid drops as well as solid particles have been observed.¹⁹

A recent calculation²⁰ of the temperature profile in the high- T_c superconductor target irradiated by laser pulses of triangular shape shows no subsurface thermal peak which is crucial to the subsurface explosion. The target surface is, however, simply specified in Ref. 20 by the melting temperature, and all parameters are assumed to be temperature independent. A more careful calculation²¹ shows the existence of subsurface overheating spots. On the other hand, subsurface thermal peaks do exist and have been observed in other materials.^{22,23} There is certainly no evidence showing why the subsurface explosion can not occur in high- T_c superconductors.

We consider in this paper a YBCO target exposed to laser pulses of different shapes and intensities, as shown in Fig. 1, and study its evaporation. We attempt to calculate the temperature profile inside the

material and its variation with the pulse shape and intensity. As the target surface is receding during the evaporation process, we solve the equations in the frame that moves with the surface. Temperature-dependent parameters are determined by extrapolation to high temperatures from the empirical formula constructed on the basis of experimental data.

II. Method of calculation

When the superconducting target material is irradiated by an intense laser pulse, its surface layers are heated continuously until the outer surface reaches the vaporization temperature T_v . Then the material is removed from the target surface in the form of electrons and positive ions, molecular clusters or solid particles. Due to further absorption of energy from the laser, the energy absorbed by the target forms a distributed heat source around its surface region, and this region is mobile because of the laser evaporation. Our problem is to study the motion of this vapor-solid interface^{18,20,23} and the temperature distribution into the target material.

During the laser irradiation, the temperature $T(x,t)$ in the material is a function of both the time t and position $x \geq X$, where X is the depth from which material has been removed by the laser. The lateral rate of heat diffusion is assumed to be small in our treatment. This function is determined by the heat diffusion equation

$$\rho(T) C_p(T) \frac{\partial}{\partial t} T(x,t) = \alpha(T)b(T)I(t)e^{-b(T)(x-X)} + \kappa(T) \frac{\partial^2}{\partial x^2} T(x,t), \quad (1)$$

where we have assumed the most general temperature-dependent parameters, namely the density ρ , specific heat C_p , thermal conductivity κ and absorption coefficient b . I is the time-dependent laser intensity, and the function $\alpha(T)$ is introduced to account for the reflection loss of the

surface and the screening effect of the vaporized material. This is necessary because the vaporized material from the target absorbs part of the laser energy and hence reduces the energy the target can absorb. The energy balance at the interface requires that the energy given to the vaporized material is equal to the heat energy flow to the surface, that is,

$$\rho(T)L_v \frac{\partial X}{\partial t} = \kappa(T) \frac{\partial}{\partial x} T(x,t) \Big|_{x=X} \quad (2)$$

where L_v is the vaporization heat.

The temperature-dependent parameters plus time-dependence of the laser intensity make it extremely difficult, if not impossible, to solve Eqs. (1) and (2) analytically. Before we proceed to solve these equations numerically, we first transform them into dimensionless forms by introducing the following variables: $\theta = T/T_v$, $\tau = t/t_0$, $S = (x-X)/\ell_0$, $L = \rho L_v$, $C = \rho C_p$ and $B = I b t_0 / C T_v$. We have chosen in these definitions $t_0 = 30$ ns, a typical laser pulse duration and $\ell_0 = 3 \times 10^{-4}$ cm. The laser intensity is measured in the unit of 1.27×10^8 W/cm². The parameter B is introduced just for convenience. Thus, Eqs. (1) and (2) become

$$\frac{\partial \theta}{\partial \tau} - u \frac{\partial \theta}{\partial S} - \frac{\kappa}{C} \frac{t_0}{\ell_0^2} \frac{\partial^2 \theta}{\partial S^2} = \alpha B e^{-b \ell_0 S} \quad (3)$$

$$u = \begin{cases} 0 & \theta < 1 \\ \left[\frac{\kappa t_0 T_v}{-v \ell_0^2} \frac{\partial \theta}{\partial S} \right]_{S=0} & \theta = 1 \end{cases} \quad (4)$$

where u stands for the speed of the moving interface. Equation (4) indicates the fact that the interface does not move until the surface

temperature reaches the vaporization temperature T_v , or $\theta = 1$. The initial temperature of the material is assumed to be the room temperature, namely, $\theta(S, 0) = 300K/T_v$. There is also a boundary condition that deep inside the solid, $S \rightarrow \infty$, the temperature remains the room temperature at any finite time. Hence, $\theta(\infty, t) = 300K/T_v$. The characteristic parameters of the material at high temperatures, however, have never been measured, at least to the best of our knowledge. Therefore we have to determine the temperature dependence of the parameters empirically from the available data before we can carry out the numerical work.

For the 1:2:3 material, we construct the approximate formulas from large amount of experimental data²⁴⁻²⁸ by the extrapolation method. According to the experimental curves given in Ref. 24, we find by extrapolation that the thermal conductivity can approximately represented by the formula

$$\kappa = 0.042 + \lambda \Delta T \quad (5)$$

in the unit of W/K-cm, where $\Delta T = T - 300K$ and $\lambda = 1.2 \times 10^{-5} W/K^2 cm$. The density is a linear function of T according to Ref. 25. The determination of the specific heat is more complicated. From the thermal expansion coefficients in Ref. 26 and the measured data of the density,²⁷ we can deduce the relation between ρ and T . The temperature dependence of C_p can be deduced from Ref. 28, and finally we find

$$C = 1.82 + 2.6 \times 10^{-8} \Delta T \quad (6)$$

in the unit of J/g-K. The absorption coefficient is a result of extrapolation of the data presented in Ref. 27, namely,

$$b = 2.27 \times 10^5 (1 - 9 \times 10^6 \Delta T) \quad (7)$$

in the unit of cm^{-1} . For the screening factor we take $\alpha = 0.9$ for $\theta < 1$ or before the vaporization starts, and $\alpha = 0.3$ when the vaporization begins ($\theta = 1$). This choice agrees with the experiment.²⁹ It is noted that the boiling temperature is still not known. A rough estimate²⁰ is twice the melting temperature, which is about³⁰ 1300K. We take $T_v = 3000\text{K}$ in our computation. We have in fact found that a change of T_v within the range³¹ of 2000 ~ 3000K does not change the result qualitatively.

III. Results and discussion

The temperature change with the depth into the material is calculated for various intensities of incident laser pulses. For all pulse shapes we have considered, it is possible to find subsurface temperatures higher than the surface temperature for sufficiently high intensity of the pulsed laser. This means that internal explosions are possible and hence provides a reasonable explanation of the observed liquid droplets and small solid particles.¹⁹ The subsurface overheating phenomenon can be understood as the penetration of the laser field into the material and the creation of heat sources therein. On the other hand, the rate of heat dissipation on the surface is much greater than that in the interior because of the surface evaporation.

Temperature profiles calculated for different cases are plotted in Figs. 2-5, and the corresponding interface receding velocity in each case is listed as a function of time in Table 1. For a rectangular pulse, the laser intensity remains constant. The interface receding acceleration increases at first and then decreases, and the subsurface peak temperature also shows

saturation. This is because the rate of thermal diffusion is proportional to the temperature gradient. The situation is depicted in Fig. 2(a) and Table 1(a). Figure 2(b) and Table 2(b) show the results for a triangular pulse. As the laser intensity increases with time until its peak, the interface receding speed also increases. As a result, the subsurface thermal peak moves into the material continuously with increasing peak temperature. In other words, the saturation phenomena are not apparent because the laser intensity keeps increasing.

To see how the time spread of laser pulses of the same peak intensity affect the temperature distribution, we take the triangular pulse as an example. We consider an ideal case in which the pulse heats the interface up to its vaporization temperature T_v as the intensity increases linearly with time and reaches its peak. Now we let the pulse intensity decrease at different rates by assuming $d = 1$ and 0.17 in Fig. 1(b). The results are plotted in Fig. 3. It is observed that in Fig. 3(a) and Table 1(c) the subsurface thermal peak still exists. The peak temperature ($\theta = 1.08$) is considerably lower than in Fig. 2(a) ($\theta = 1.7$) because the laser peak intensity has been reduced from unity to 0.28 . The interesting point is that even if the laser intensity decreases linearly with time, the peak temperature is still increasing with time during $0 < \tau \leq 0.24$ and the peak position keeps moving inward. After that time or $\tau \geq 0.24$, the peak is stable, indicating energy balance at that point, that is, heat supplied by the laser pulse merely compensates that dissipated by diffusion. The interface receding speed increases with time first, reaches its maximum and then decreases.

If the triangular pulse shape is such that the intensity drops off quickly after its peak, the subsurface temperature peak disappears. As can be seen in Fig. 3(b) and Table 1(d), the temperature decreases monotonically with the depth into the material, and consequently the internal explosion can not occur.

Since the shape of laser pulses in practical uses is more Gaussian-like, we now consider a pulse with intensity

$$I(t) = I_{\max} \exp(-t^2/2\sigma^2), \quad (8)$$

where σ is a parameter characterizing the width of the pulse, and I_{\max} is the peak intensity. Numerical results for a YBCO target with a pulse of ~30 ns long are shown in Fig. 4. The curves in Fig. 4(a) illustrate clearly the subsurface overheating at different instants as long as the pulse intensity is sufficiently strong. This implies that internal explosion occurs in the laser ablation process if the pulse intensity is strong enough, and hence provides a theoretical basis for a hypothetical explanation of the observed solid particles.¹⁹ The formation of such subsurface overheating spots can be controlled by reducing the laser intensity.

According to parameters reported in Ref. 5, the maximum laser intensity I_{\max} is estimated to be $\sim 0.7 \times 10^8 \text{ W/cm}^2$, which falls within the range of intensity for the appearance of subsurface overheating in Fig. 4(a). The temperature peaks decrease as the pulse intensity decreases. They eventually disappear for $I_{\max} \leq 0.13 \times 10^8 \text{ W/cm}^2$, which may be regarded as a threshold intensity for the subsurface overheating under experimental conditions described by the same parameters.

Corresponding to every instant in Fig. 4, the target surface receding velocities for all the cases can be calculated and are listed in Table 1. By comparison, we find that the receding velocity and the pulse intensity reach their peaks almost simultaneously for high laser intensities. On the other hand, the laser intensity reaches its peak before the receding velocity for weaker pulses, as expected.

In order to avoid the undesirable products of internal explosion, the pulse intensity has to be reduced. Excessive reduction of the laser intensity, however, is not desirable either, because the evaporation rate may become too low to be practical. A good choice is probably just above the threshold intensity, as found in Fig. 4(c) for the present case. It should be emphasized from the above discussions that the pulse shape can also make an important difference, especially when the intensity is strong. In Fig. 5, we compare a sine wave with the Gaussian of the same peak intensity. The difference is not very significant because I_{\max} is not strong. In conclusion, we find that the most efficient deposition requires pulse shapes with a quickly diminishing tail after its peak, such as a narrow Gaussian pulse.

Acknowledgments

This work was supported in part by the New York State Institute on Superconductivity and in part by Office of Naval Research.

References

1. K. Char, A.D. Kent, A. Kapitulnik, M.R. Beasley and T.H. Geballe, Appl. Phys. Lett. 51, 1370 (1987).
2. R.B. Laibowitz, R.H. Koch, P. Chaudhari and R.J. Gambino, Phys. Rev. B 35, 8821 (1987).
3. J. Kwo, T.C. Hsieh, R.H. Fleming, M. Hong, S.H. Liou, B.A. Davidson and L.C. Feldman, Phys. Rev. B 36, 4089 (1987).
4. C.E. Rice, R.B. van Dover and G.J. Fisanick, Appl. Phys. Lett. 51, 1842 (1987).
5. D. Dijkkamp, T. Venkatesan, X.D. Wu, S.A. Shaheen, N. Jisrawi, Y.H. Min-Lee, W.L. Mclean and M. Croft, Appl. Phys. Lett. 51, 619 (1987); J. Narayan, N. Biunno, R. Singh, O.W. Holland and O. Auciello, Appl. Phys. Lett. 51, 1845 (1987); K. Moorjani, J. Bohandy, F.J. Adrian, B.F. Kim, R.D. Shull, C.K. Chiang, L.J. Swartzendruber and L.H. Bennett, Phys. Rev. B 36, 4036 (1987).
6. X.D. Wu, X.X. Xi, Q. Li, A. Inam, B. Dutta, L. DiDomenico, C. Weiss, J.A. Martinez, B.J. Wilkens, S.A. Schwarz, J.B. Barner, C.C. Chang, L. Nazar and T. Venkatesan, Appl. Phys. Lett. 56, 400 (1990).
7. C.T. Rogers, A. Inam, M.S. Hegde, B. Dutta, X.D. Wu and T. Venkatesan, Appl. Phys. Lett. 55, 2032 (1989).
8. R. Ramesh, A. Inam, W.A. Bonner, P. England, B.J. Wilkens, B.J. Meagher, L. Nazar, X.D. Wu, M.S. Hegde, C.C. Chang and T. Venkatesan, Appl. Phys. Lett. 55, 1138 (1989).
9. S. Witanachchi, H.S. Kwok, X.W. Wang and D.T. Shaw, Appl. Phys. Lett. 53, 234 (1988).

10. D.T. Shaw, S. Witanachchi and H.S. Kwok, U.S. Patent # 4,874,741; also see Quarterly Report, New York State Institute on Superconductivity, Vol. 1, No. 1, ~~PR. 3~~ (1990).
11. T. Venkatesan, X.D. Wu, A. Inam and J.B. Wachtman, Appl. Phys. Lett. 52, 1193 (1988).
12. R.K. Singh, N. Biunno and J. Narayan, Appl. Phys. Lett. 53, 1013 (1988).
13. W.A. Weimer, Appl. Phys. Lett. 52, 2171 (1988).
14. J.P. Zheng, Z.Q. Huang, D.T. Shaw and H.S. Kwok, Appl. Phys. Lett. 54, 280 (1989).
15. C.H. Becker and J.B. Pallix, J. Appl. Phys. 64, 5152 (1988); K.L. Saenger, *ibid.*, 66, 4435 (1989).
16. D.B. Geohegan, D.N. Mashburn, R.J. Culbertson, S.J. Pennycook, J.D. Budai, R.E. Valiga, B.C. Sales, D.H. Lowndes, L.A. Boatner, E. Sonder, D. Eres, D.K. Christen and W.H. Chrislie, J. Mat. Res. 3, 1169 (1988).
17. R.K. Singh and J. Narayan, Phys. Rev. B 41, 8843 (1990); R.K. Singh, O.W. Holland and J. Narayan, J. Appl. Phys. 68, 233 (1990).
18. F.W. Dabby and U. Paek, IEEE J.Q.E, QE 8, 106 (1972).
19. T. Vankatesan, C.C.Chang, D. Dijkkamp, S.B. Ogale, E.W. Chase, L.A. Farrow, D.M. Hwang, P.F. Miceli, S.A. Schwarz, J.M. Tarascon, X.D. Wu and A. Inam, J. Appl. Phys. 63 4591 (1988).
20. A.N. Jette and W.J. Green, J. Appl. Phys. 68, 5273 (1990).
21. D.L. Lin, Z.D. Liu, X. Li and T.F. George, unpublished.
22. F.P. Gagliano and U.C. Paek, Appl. Opt. 13, 274 (1974).
23. R.K. Singh, D. Bhattacharya and J. Narayan, Appl. Phys. Lett. 57, 2022 (1990).

24. C. Uher, in Superconductivity and Applications, ed. by H.S. Kwok, Y.H. Kao and D.T. Shaw, (Plenum, New York, 1990), pp. 217 ~~88~~.
25. J. Heremans, D.T. Morelli, G.W. Smith and S.C. Slrite, Phys. Rev. B 37, 1604 (1988).
26. H.M. Obryan and P.K. Gallagher, Mat. Res. Soc. Symp. Proc. 169, 1093 (1990).
27. A. Inam, X.D. Wu, T. Venkatesan, S.B. Ogale, C.C. Chang and D. Dijkkamp, Appl. Phys. Lett. 51, 1112 (1987).
28. A. Junod, Physica C 153-155, 1078 (1988).
29. F. Lu, C.H. Perry, K. Chen, R.S. Markiewicz, Mat. Res. Soc. Symp. Proc. 169, 1009 (1990); T. Timusk and D.B. Tanner, in Physical Properties of High Temperature Superconductors, ed. by D.M. Ginsberg (World Scientific, Singapore, 1989).
30. T. Terashima, K. Iijima, K. Yamamoto, Y. Bando and H. Mazaki, Jpn. J. Appl. Phys. 27, 191 (1988).
31. R.S. Roth, K.L. Davis and J.R. Dennis, Adv. Ceramic Mat. 2 303 (1987).

Figure captions

1. Laser pulse shapes considered in this paper. The intensity and duration are measured in the numerical work by $1.27 \times 10^8 \text{ W/cm}^2$ and 30 ns, respectively. (a) Rectangular pulse, (b) Triangular pulse, (c) Gaussian pulse, (d) Sinusoidal pulse.

2. Temperature profile as a function of the depth $x-X$ (in 60 Å) into the kat material at different instants (t is in the unit of 30 ns). The switch-on time of the laser pulse is taken to be $t = 0$. Curve 1 is for the moment when the surface temperature just reaches T_v ; 2 is for $t = 0.08$; 3 is for $t = 0.16$; 4 is for $t = 0.24$; 5 is for $t = 0.32$; and 6 is for $t = 0.40$. (a) Triangular pulse with $a = 1$, $c = 0.4$ and $d = 0$. (b) Rectangular pulse with $a = 1$ and $b = 0.4$.

3. Subsurface temperature versus the depth $x-X$ at different instants under irradiation of a triangular pulse with $a = 0.28$, $c = 0.028$ and (a) $d = 1$, (b) $d = 0.17$. Otherwise, all curves are the same in Fig. 2.

4. Subsurface temperature versus the depth $x-X$ at different instants for a Gaussian pulse with $a = 0.25$ and $b = 1$. Curve 1 is for the moment when the surface just reaches T_v ; 2 is for $t = 0.2$; 3 is for $t = 0.35$; 4 is for $t = 0.5$; 5 is for $t = 0.65$; and 6 is for $t = 0.8$.

5. Subsurface temperature versus the depth $x-X$ at different instants for a (a) Gaussian and (b) sinusoidal pulse, both with $a = 0.2$ and $b = 1$. Curve 1 is for the moment when the surface temperature reaches T_v ; 2 is for $t = 0.35$; 3 is for $t = 0.5$; and 4 is for $t = 0.65$.

Table 1: Interface receding velocity at different instants for laser pulse shapes given in Fig. 1.

$t \times 30 \text{ ns}$	Receding velocity $v \times 10^3 \text{ cm/s}$			
	(a)	(b)	(c)	(d)
0.08	-	-	13.7	5.7
0.16	0.37	1.29	24.5	0
0.24	0.71	1.34	22.6	0
0.32	1.02	1.37	21.6	0
0.40	1.32	1.39	19.7	0

Fig. 1

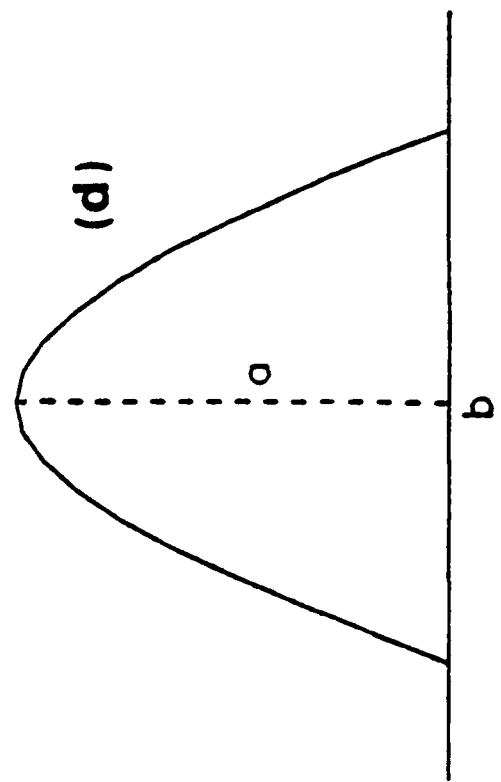
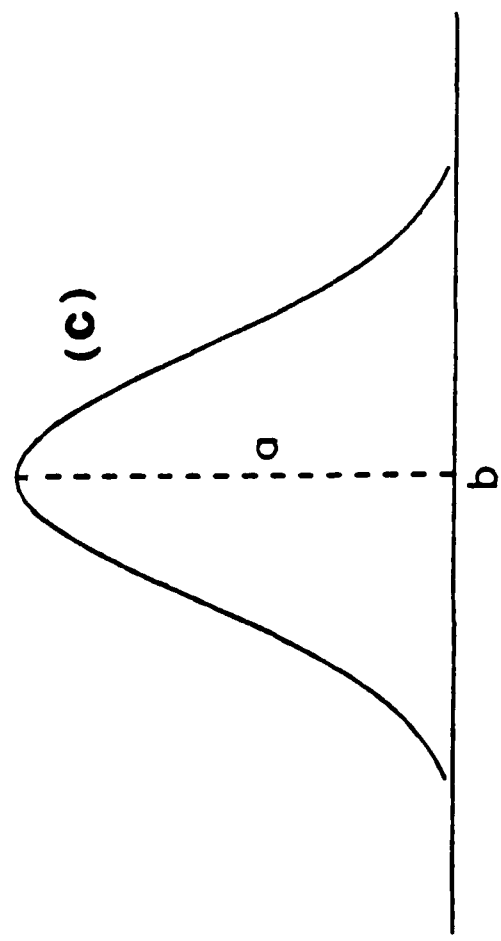
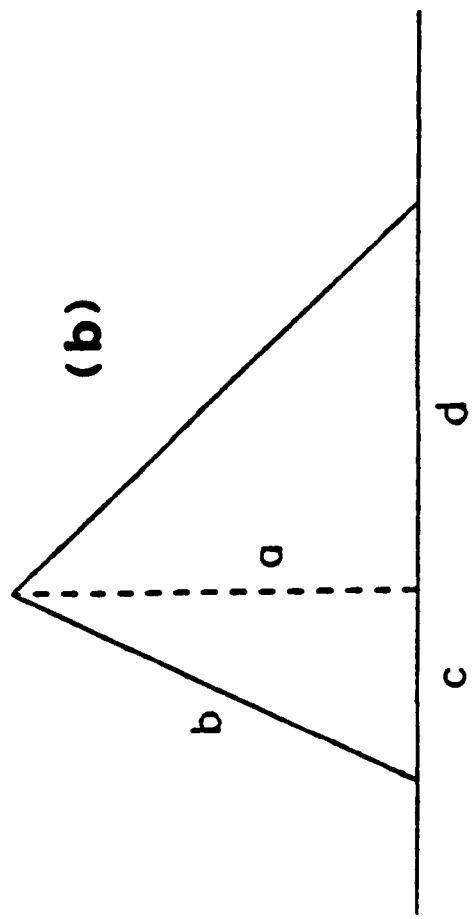
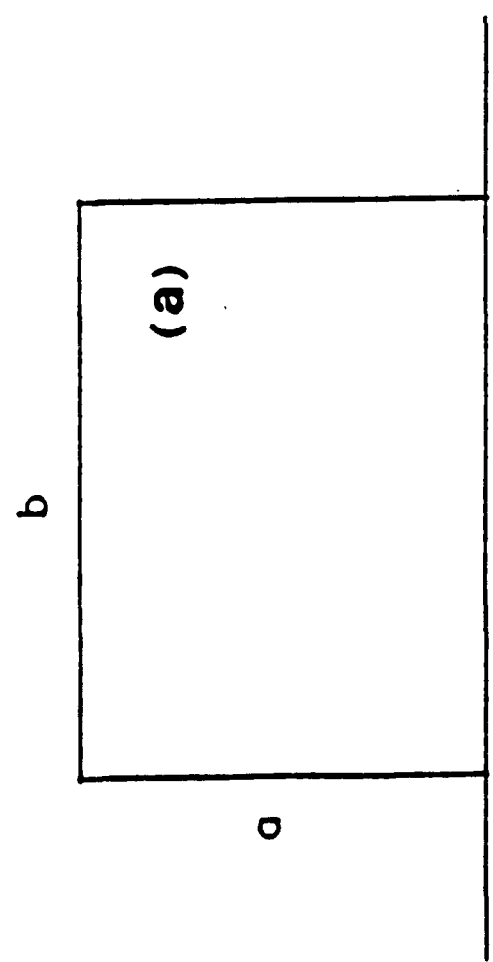


Fig. 2

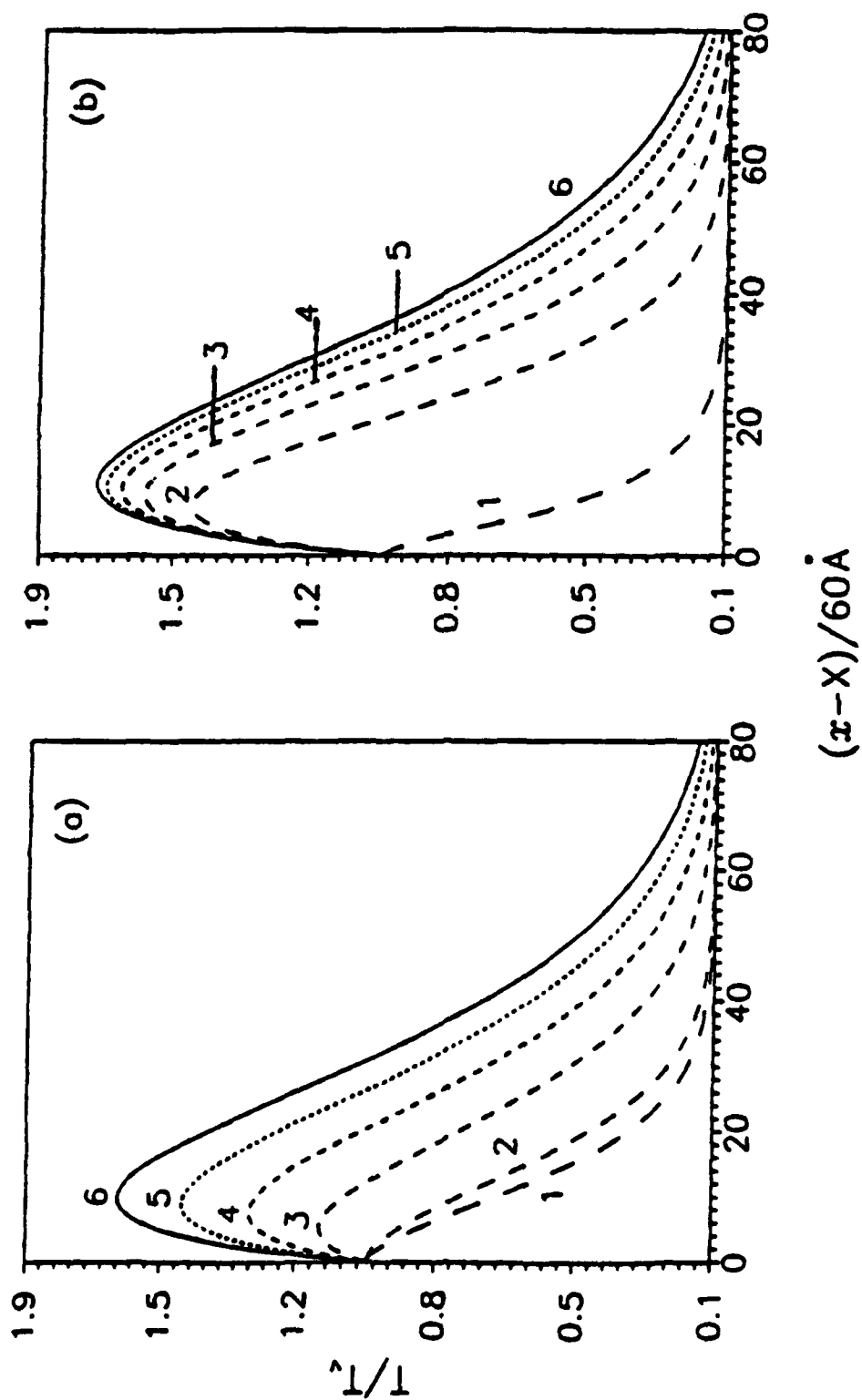


Fig. 3

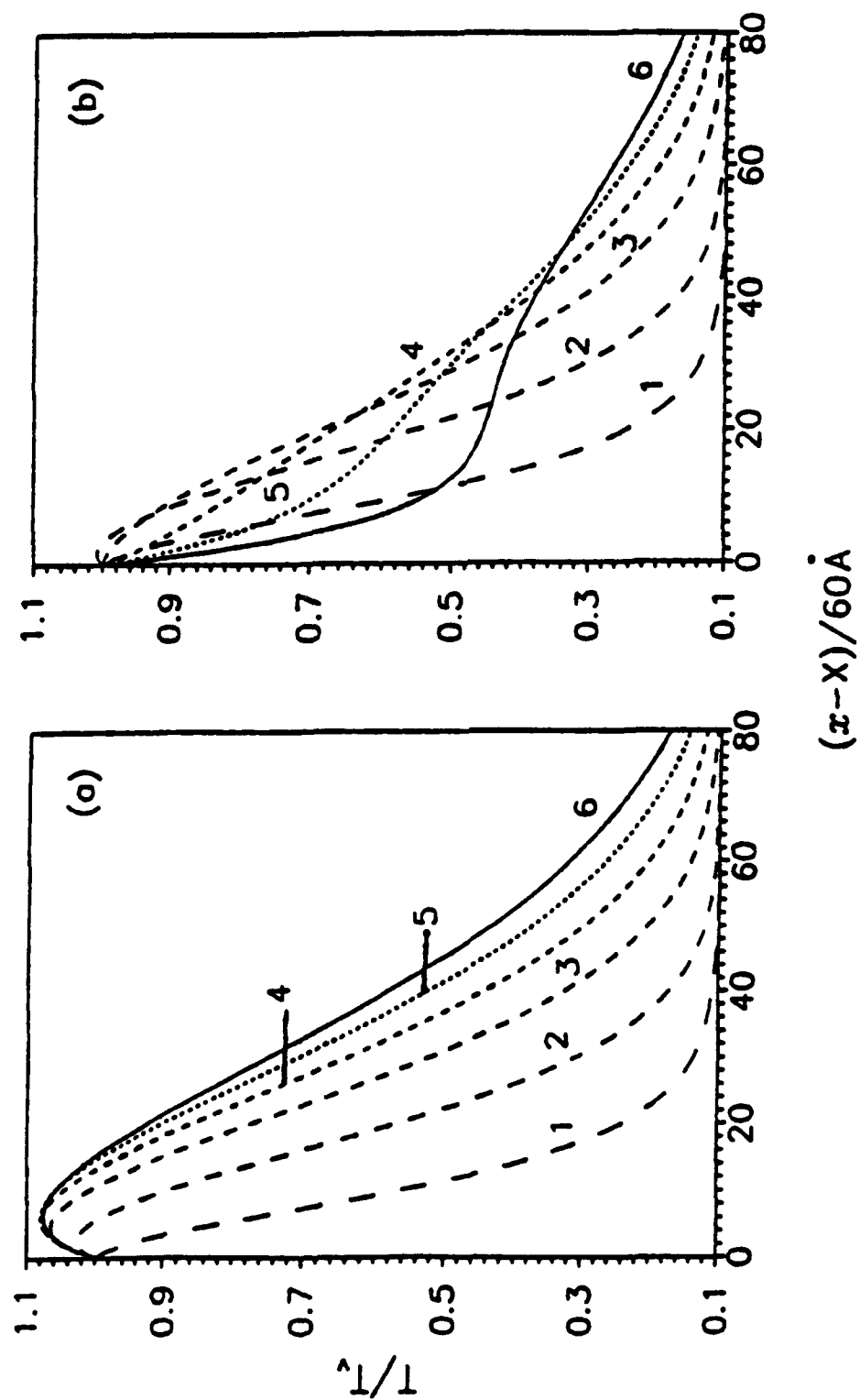


Fig. 4

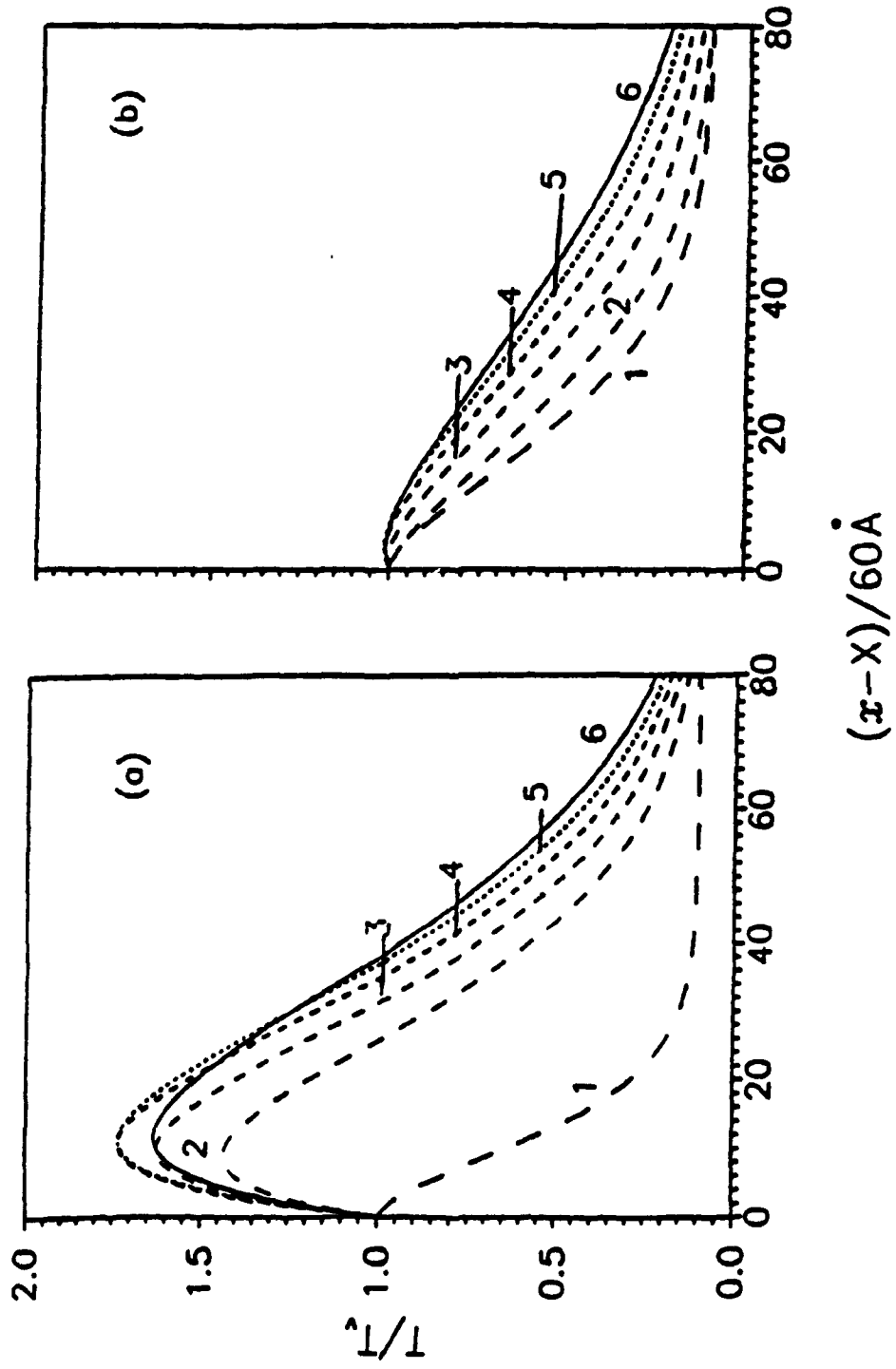


Fig. 5

